



Universiteit
Leiden
The Netherlands

Molecular analysis of the HPJ-JT syndrome and sporadic parathyroid carcinogenesis

Haven, C.J.

Citation

Haven, C. J. (2008, May 28). *Molecular analysis of the HPJ-JT syndrome and sporadic parathyroid carcinogenesis*. Retrieved from <https://hdl.handle.net/1887/12960>

Version: Corrected Publisher's Version

License: [Licence agreement concerning inclusion of doctoral thesis in the Institutional Repository of the University of Leiden](#)

Downloaded from: <https://hdl.handle.net/1887/12960>

Note: To cite this publication please use the final published version (if applicable).

Chapter 3

HRPT2, encoding parafibromin, is mutated in hyperparathyroidism-jaw tumor syndrome.

Nat. Genet. 2002 Dec;32(4):676-80. Epub 2002 Nov 18.

letter

HRPT2, encoding parafibromin, is mutated in hyperparathyroidism–jaw tumor syndrome

J.D. Carpten¹, C.M. Robbins¹, A. Villablanca^{2,3}, L. Forsberg^{2,4}, S. Presciutti⁵, J. Bailey-Wilson⁵, W.F. Simonds⁶, E.M. Gillanders¹, A.M. Kennedy⁷, J.D. Chen⁸, S.K. Agarwal⁶, R. Sood¹, M.P. Jones¹, T.Y. Moses¹, C. Haven⁹, D. Petillo⁸, P.D. Leotlela⁷, B. Harding⁷, D. Cameron¹⁰, A.A. Pannett⁷, A. Höög³, H. Heath III¹¹, L.A. James-Newton⁶, B. Robinson¹², R.J. Zarbo¹³, B.M. Cavaco¹⁴, W. Wassif¹⁵, N.D. Perrier⁶, I.B. Rosen¹⁶, U. Kristoffersson¹⁷, P.D. Turnpenny¹⁸, L.-O. Farnebo⁴, G.M. Besser¹⁹, C.E. Jackson²⁰, H. Morreau⁹, J.M. Trent¹, R.V. Thakker⁷, S.J. Marx⁶, B.T. Teh⁸, C. Larsson^{2,8} & M.R. Hobbs²¹

Published online 18 November 2002; doi:10.1038/ng1048

We report here the identification of a gene associated with the hyperparathyroidism–jaw tumor (HPT–JT) syndrome. A single locus associated with HPT–JT (*HRPT2*) was previously mapped to chromosomal region 1q25–q32. We refined this region to a critical interval of 12 cM by genotyping in 26 affected kindreds. Using a positional candidate approach, we identified thirteen different heterozygous, germline, inactivating mutations in a single gene in fourteen families with HPT–JT. The proposed role of *HRPT2* as a tumor suppressor was supported by mutation screening in 48 parathyroid adenomas with cystic features, which identified three somatic inactivating mutations, all located in exon 1. None of these mutations were detected in normal controls, and all were predicted to cause deficient or impaired protein function. *HRPT2* is a ubiquitously expressed, evolutionarily conserved gene encoding a predicted protein of 531 amino acids, for which we propose the name parafibromin. Our findings suggest that *HRPT2* is a tumor-suppressor gene, the inactivation of which is directly involved in predisposition to HPT–JT and in development of some sporadic parathyroid tumors.

Parathyroid tumors affect 1 in 1,000 individuals in the general population in whom the resulting primary hyperparathyroidism (1°HPT) occurs as the only clinical feature or as part of a complex syndrome. The HPT–JT syndrome (OMIM *145001) is an autosomal dominant, multiple neoplasia syndrome primarily characterized by hyperparathyroidism due to parathyroid tumors^{1,2}. Thirty percent of individuals with HPT–JT may also develop ossifying fibromas, primarily of the mandible and maxilla, which are distinct from the 'brown' tumors associated with severe hyperparathyroidism^{1,3–5}. Kidney lesions may also occur

in HPT–JT as bilateral cysts, renal hamartomas or Wilms tumors^{2,5–7}. Linkage analysis previously assigned the locus associated with HPT–JT (*HRPT2*) to a region of roughly 15 cM within 1q24–q32 (refs 5,6,8). Some parathyroid carcinomas and renal hamartomas from individuals with HPT–JT, as well as some sporadic parathyroid adenomas, show somatic 1q loss of heterozygosity (LOH), in agreement with the inactivation of a tumor-suppressor gene in the region^{6,7,9–11}.

To facilitate the identification of the gene associated with HPT–JT, we studied a total of 26 kindreds, sixteen of whom have been described elsewhere and most of whom showed linkage to 1q24–q32 (refs 2,5–7,10,12–16). Twenty-four kindreds were affected with HPT–JT, and two were affected with familial isolated hyperparathyroidism (FIHP). The latter had a familial occurrence only of 1°HPT and showed linkage to 1q24–q32, but not to *MEN1*. (multiple endocrine neoplasia I; ref. 9). We genotyped 26 microsatellite markers within 1q24–q32. Key recombinants further narrowed the candidate interval to 12 cM flanked by *DIS238* and *DIS477* (Fig. 1a). Using existing transcript mapping information from this region¹⁷ and the UCSC draft human genome sequence browser, we identified 67 potential candidate genes including known genes, full-length cDNAs with no homologies to known genes, spliced expressed sequence tags (ESTs) and predicted genes. Fig. 1b shows a partial transcript map of the critical candidate region highlighting the initial set of candidate genes selected for mutational screening. We carried out mutational analysis using double-stranded DNA sequencing on a panel of 26 lymphocyte DNA samples, each representing one affected individual from each kindred.

¹Cancer Genetics Branch, National Human Genome Research Institute, National Institutes of Health, Bethesda, Maryland 20892, USA. ²Department of Molecular Medicine, ³Department of Oncology and Pathology and ⁴Department of Surgical Sciences, Karolinska Hospital, Stockholm, Sweden. ⁵Inherited Disease Research Branch, National Human Genome Research Institute, National Institutes of Health, Baltimore, Maryland, USA. ⁶Metabolic Diseases Branch, National Institute of Diabetes and Digestive and Kidney Diseases, Bethesda, Maryland, USA. ⁷Molecular Endocrinology Group, Nuffield Department of Clinical Medicine, University of Oxford, John Radcliffe Hospital, Headington, Oxford, UK. ⁸Laboratory of Cancer Genetics, Van Andel Research Institute, Grand Rapids, Michigan, USA. ⁹Department of Pathology, Leiden University Medical Center, The Netherlands. ¹⁰Department of Diabetes and Endocrinology, Princess Alexandra Hospital, Brisbane, Australia. ¹¹Eli Lilly Company, Lilly Corporate Center, Indianapolis, Indiana, USA. ¹²Kolling Institute of Medical Research, Royal North Shore Hospital, University of Sydney, Australia. ¹³Department of Pathology, Henry Ford Hospital, Detroit, Michigan, USA. ¹⁴Centro de Investigação de Patobiologia Molecular, Instituto Português de Oncologia de Francisco Gentil, Rua do Professor Lima Basto, Lisboa, Portugal. ¹⁵Department of Clinical Biochemistry, King's College School of Medicine and Dentistry, London, UK. ¹⁶Mount Sinai Hospital, Toronto, Ontario, Canada. ¹⁷Department of Clinical Genetics, University Hospital, Lund, Sweden. ¹⁸Clinical Genetics Department, Royal Devon and Exeter Hospital (Worford), Barrack Road, Exeter, UK. ¹⁹Department of Endocrinology, St Bartholomew's Hospital, London, UK. ²⁰Department of Medical Genetics, Henry Ford Hospital, Detroit, Michigan, USA. ²¹Divisions of Endocrinology & Infectious Diseases, University of Utah, Salt Lake City, Utah, USA. Correspondence should be addressed to C.L. (e-mail: Catharina.Larsson@cmm.ki.se) or J.D.C. (jdc@nhgri.nih.gov).





After analysis of sequence data from the initial set of prioritized candidate genes, only the *C1orf28* gene (Unigene cluster Hs.5722) had probable disease-causing mutations. Unigene cluster Hs.5722 is represented in cDNA libraries from all tissues of interest (parathyroid, kidney and bone), but is probably ubiquitously expressed. The *C1orf28* gene consists of 17 exons, all of which are coding (Fig. 1c). Alignment of EST and full-length cDNA sequences from Unigene cluster Hs.5722 identified an open reading frame of 1,596 nucleotides encoding a protein of 531 amino acids. The combined coding sequence data suggested a full-length message of approximately 2.7 kb for this transcript, which correlates well with the major band of roughly 2.7 kb that we detected by northern-blot analysis using the *C1orf28* coding region as a probe (Fig. 1d). Other bands present on the northern blot could represent alternative forms of the protein and are currently under investigation. Following the OMIM nomenclature for *145001, we refer to this gene as *HRPT2*.

We identified a total of 13 heterozygous germline mutations in *HRPT2* in 14 of the 26 index cases screened (Table 1). Each germline mutation in *HRPT2* is expected to lead to impaired protein function owing to truncation or premature stops, further

supporting their pathogenic importance. Inheritance of five different mutations is detailed in Fig. 2. One frameshift mutation, an insertion of 2 bp in exon 7 (Fig. 2d), was found in individuals of two independently identified, seemingly unrelated kindreds (kindred-01 and kindred-33) who were later found to share an identical disease haplotype through the entire 26-marker interval, suggesting that these individuals have a common ancestor. In all 14 affected families, all affected and some currently unaffected members of the 14 families harbored mutations. None of the mutations were present in 150 normal diploid control individuals.

HRPT2 and its encoded protein are evolutionarily conserved, as we found potentially orthologous sequences in mouse, *Drosophila melanogaster* and *Caenorhabditis elegans* in the National Center for Biotechnology Information non-redundant nucleotide database using the BLAST algorithm. We propose the name parafibromin for the encoded protein, owing to its involvement in the development of parathyroid tumors and ossifying jaw fibromas. Human parafibromin shares 54% identity and 67% similarity with the *D. melanogaster* ortholog and 25% identity and 45% similarity with the *C. elegans* ortholog (see Web Fig. A online).

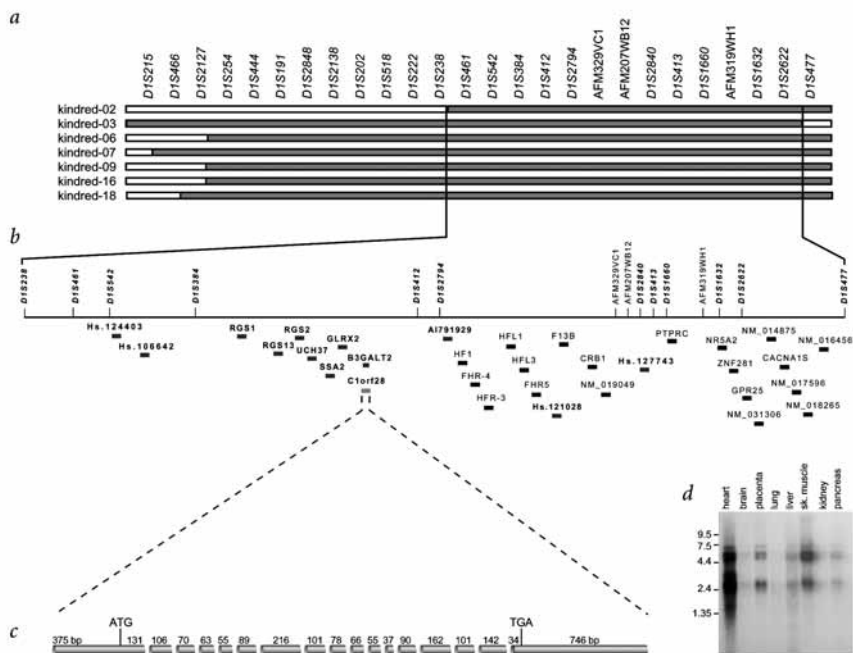


Fig. 1 Genetic analysis of kindreds affected with HPT-JT and partial transcript map of the critical region. **a**, Recombination map spanning 26 microsatellite markers from the 1q24-q32 genetic interval showing key recombination events. Marker regions shaded in red represent regions shared among affected individuals within families. **b**, A partial transcript map of the critical region defined by recombinants. Genes highlighted in blue were initially prioritized for mutational analysis. *C1orf28* is labeled in red as the gene of interest (*HRPT2*). Known genes and full-length cDNAs are shown with GenBank accession numbers, and ESTs are shown with Unigene cluster ID numbers. **c**, Genomic structure of *HRPT2*. Sizes of exons are given in base pairs (bp). ATG and TGA represent the initiation codon and termination codon, respectively, of *HRPT2*. **d**, Northern-blot analysis using *C1orf28* (*HRPT2*) as a probe. *C1orf28* (*HRPT2*) was expressed at varying levels in all tissues examined. Molecular weight markers are given in kb.

letter

Table 1 • Germline and somatic mutations detected in *HRPT2*

Kindred or tumor sample	Clinical data (number)				Mutation in <i>HRPT2</i>		Coding change	Type
	HPT	PTC	JT	KL	Location	Nucleotide change		
Mutations in kindreds affected with HPT-JT								
kindred-05	4	0	2	4	exon 1	3G→A	Met11Ileu	germline
kindred-15	7	0	3	1	exon 1	25C→T	Arg9X	germline
kindred-16	7	2	5	0	exon 1	41-bp duplication/insertion	frameshift	germline
kindred-24	2	0	1	1	exon 1	34delAACATCC	frameshift	germline
kindred-12	4	0	3	0	exon 1	30delG	frameshift	germline
kindred-19	2	1	2	0	exon 1	39delC	frameshift	germline
kindred-10	6	1	5	4	exon 2	165C-G	Tyr55X	germline
kindred-20	7	1	2	1	exon 3	*306delGTgtgagtactttt	frameshift / splice mutation	germline
kindred-09	10	3	0	0	exon 4	356delA	frameshift	germline
kindred-22	3	0	2	1	exon 5	406A→T	Lys136X	germline
kindred-07	4	0	2	2	exon 7	636delT	frameshift	germline
kindred-01	5	3	0	3	exon 7	679insAG	frameshift	germline
kindred-33	2	0	1	0	exon 7	679insAG	frameshift	germline
kindred-11	3	0	2	1	exon 14	1238delA	frameshift	germline
Mutations in parathyroid tumors								
tumor sample 9	sporadic				exon 1	126del24	frameshift / splice mutation	somatic
tumor sample 10	FIHP-1q linked				exon 1	128G→A	Trp43X	somatic
tumor sample 31	sporadic				exon 1	53delT	frameshift	somatic

Nucleotide and amino-acid positions start from initiation codon. *Lower case nucleotides represent intronic sequences. HPT, hyperparathyroidism; PTC, parathyroid carcinoma; JT, jaw tumor; KL, kidney lesion.

There were no homologies to known protein domains, but moderate identity (32%) and similarity (54%) to a protein of *Saccharomyces cerevisiae* known as Cdc73p, which is an accessory factor associated with an alternative RNA polymerase II important in transcriptional initiation and elongation in yeast¹⁸⁻²⁰.

To evaluate further the probable tumor-suppressor effect of *HRPT2*, we analyzed LOH and screened for mutations in *HRPT2* in tumor and normal DNA from 48 individuals with parathyroid adenomas with cystic features (47 sporadic and 1 familial). Six sporadic tumor samples (12.5%) showed LOH at 1q without involvement of 11q13, two with LOH at 1q encompassing the *HRPT2* locus. We identified a total of three inactivating mutations in *HRPT2*, two in sporadic tumors and one in a tumor from a 1q-linked FIHP kindred. Details on mutations and LOH at 1q for the three tumor samples can be found in Table 1 (also see Web Fig. B online). None of the mutations were detected in adjacent normal tissue or in 150 normal diploid control individuals, suggesting that they were pathogenic for these tumors.

LOH at 1q has been previously reported in tumors from kindreds affected with HPT-JT in whom we identified germline mutations in this study, including kindred-07, kindred-09, kindred-10 and kindred-20, suggesting that biallelic inactivation of *HRPT2* is associated with HPT-JT^{6,10,15}. These findings are in agreement with inactivation of a tumor-suppressor gene in the region. But the frequency of demonstrated LOH at 1q in parathyroid tumors related to HPT-JT is relatively low, especially compared with LOH of *MEN1*, which is inactivated in more than 70% of the associated parathyroid tumors²¹⁻²³. Our demonstration of a somatic inactivating mutation in a parathyroid adenoma from a kindred affected with FIHP that showed linkage to 1q indicates that small mutations in *HRPT2* could be one explanation for the relative lack of LOH at 1q in parathyroid tumors related to HPT-JT. Other possible mechanisms for inactivation of *HRPT2* include hypermethylation and regulatory inactivation.

The identification of deleterious disease-associated germline mutations in *HRPT2* in 14 kindreds affected with HPT-JT indicates that this gene is directly associated with the pathogenesis of the HPT-JT syndrome. Somatic inactivating mutations in parathyroid tumors suggest an important role for *HRPT2* in

parathyroid tumorigenesis. With the identification of *HRPT2*, the primary gene involved in each of the complex syndromes associated with 1stHPT is now known²⁴. This finding is expected to be of clinical relevance for early risk assessment in individuals from families with HPT-JT and possibly a subset of individuals with FIHP. As parathyroid tumors are malignant at a higher frequency in HPT-JT than in MEN1 and MEN2, mutations in *HRPT2* are probably an important precursor for increased risk of parathyroid carcinoma. Further experimentation is also warranted to determine the actual role of parafibromin in normal cellular function and the exact mechanisms by which abnormal parafibromin leads to the development of tumors. In conclusion, the identification of *HRPT2* and further analysis of parafibromin may ultimately contribute to understanding parathyroid tumor development, and eventually to the development of novel therapies for 1stHPT and, possibly, other neoplasms.

Note added in proof: Recent analyses of additional members of kindred 08, an FIHP kindred, has identified a germline L64P mutation in exon 2 of *HRPT2*.

Methods

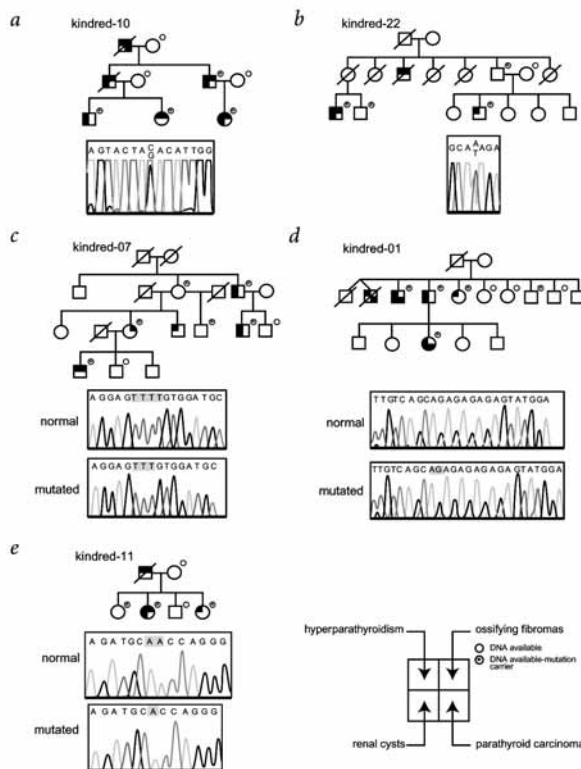
Linkage analysis and recombination mapping. All samples used in this study were collected with proper consent and approved for study by institutional review boards and ethics committees at all affiliated institutions. We genotyped genomic DNA samples using 26 short tandem-repeat microsatellite markers in the region of interest of chromosome 1. Primer sequences for the microsatellite repeat markers used in this study are available upon request. PCR reactions were set up using a TECAN Genesis200 robot. PCR amplification was done in 15-µl reactions using GeneAmp 9600 thermocyclers (PE/Applied Biosystems). Depending on the PCR yield, we pooled 5–15 µl of PCR product from up to 12 individual markers of appropriate size and fluorescent label. We separated PCR products using the ABI 377 DNA sequencer (PE/Applied Biosystems), which allows multiple fluorescently-labeled markers to be co-electrophoresed in a single lane. We used the ROX 400 size standard as an internal size-standard in each lane (PE/Applied Biosystems). We calculated allele sizes using the local southern algorithm available in the GENESCAN software program (PE/Applied Biosystems). Allele calling and binning was done using the GENOTYPER software (PE/Applied Biosystems). We included a control individual (CEPH 1347-02) in the genotyping analysis for quality control.

Fig. 2 Mutations in kindreds affected with HPT-JT. Shaded upper left quadrant represents hyperparathyroidism, upper right quadrant represents ossifying fibroma of the jaw, lower left quadrant represents renal cysts or other kidney tumors, and lower right quadrant represents parathyroid carcinoma. A line drawn through a symbol represents a deceased individual. Completely open symbols represent individuals who are currently unaffected. Small superscript circles to the upper right of family member symbols represent those individuals for whom DNA was available for mutational analysis. Small superscript circles with an asterisk (*) in the middle represent those individuals who are confirmed mutation carriers. **a**, Kindred-10 and chromatogram showing the heterozygous 165C→G nonsense mutation in exon 2. **b**, Kindred-22 and chromatogram showing the heterozygous 406A→T nonsense mutation in exon 5. **c**, Kindred-07 and chromatograms showing the normal allele and corresponding 636delT mutated allele in exon 7. **d**, Kindred-01 and chromatograms showing the normal allele and corresponding 679insAG mutated allele in exon 7. **e**, Kindred-11 and chromatograms showing the normal allele and corresponding 1238delA mutated allele in exon 14. For **c-e**, PCR products from single affected individuals carrying mutations were subcloned and subsequently sequenced to obtain sequences for both the mutated and normal alleles from the same individual.

We created the genetic map of the typed markers using the GAS package version 2.3, applying the genetic model previously used⁵. We identified critical recombinants by constructing affected haplotypes using GeneHunters²⁵, after inspecting the pedigrees to check that the program had enough information for this task.

PCR amplification and sequencing of germline mutations. We determined the genomic structures for candidate genes and designed primers from intronic sequence flanking coding exons (primer sequences are available upon request). We added M13 tails to all PCR primers for subsequent sequence analysis.

We carried out PCR reactions for individual exons in 50- μ l reaction volumes containing 20 ng of genomic DNA, PCR buffer (Invitrogen Life Technologies), 2.25 mM Mg²⁺, 250 nM dNTPs, 10 pmol forward/reverse primer mix, 0.06 unit Platinum Taq DNA polymerase (Invitrogen Life Technologies) and 0.06 unit AmpliTaq Gold (PE Biosystems). PCR cycles consisted of an initial denaturation at 94 °C for 12 min; 10 cycles of 94 °C for 20 s, annealing for 20 s and 72 °C for 20 s; then 25 cycles of 89 °C for 20 s, annealing for 20 s and 72 °C for 20 s; and a final extension at 72 °C for 10 min. Annealing temperatures were optimized for all primer sets, and this information is available upon request. We analyzed a 5 μ l aliquot of PCR product from each reaction on 2% agarose gels to determine robustness of amplification. PCR amplicons were purified using the QiaQuick PCR purification kit on the BioRobot 8000 Automated Nucleic Acid Purification and Liquid Handling system (Qiagen). We carried out double-stranded sequencing using quarter-volume cycle-sequencing reactions prepared in 96-well format using standard M13 forward or reverse primers with the BigDye Terminator Chemistry (PE/Applied Biosystems). After Sephadex purification, we separated sequence products on a 3700 Capillary DNA Analyzer (PE/Applied Biosystems) using manufacturer's protocols. We aligned and analyzed sequence chromatograms using Sequencer version 4.1 (Gene Codes). For PCR products containing potential frameshift mutations, we subcloned PCR products from affected individuals using the TOPO TA cloning system (Invitrogen Life Technologies) according to the manufacturer's recommendations. Positively selected subclones were grown in 3 ml of Luria-Bertani broth supplemented with the appropriate antibiotic selection. We prepared DNA from subclones using the Qiagen Miniprep



Plasmid Purification System. We sequenced plasmid DNA with the standard T7 and M13 reverse primers using BigDye Terminator Chemistry (PE/Applied Biosystems). We separated and analyzed samples as described above.

Northern-blot analysis. To determine the transcript size(s) and tissue distribution pattern of *HRPT2*, we hybridized PCR products spanning the coding region of the *HRPT2* mRNA sequence to a commercially available multiple-tissue northern blot, MTN1 (Clontech). The probes were labeled with α -³²P-dCTP by random priming (Stratagene) following the manufacturer's recommendations. We carried out hybridization at 42 °C overnight in Hybrisol 1 hybridization buffer (InterGen) followed by stringent washing. We then subjected filters to autoradiography.

Detection of mutations in *HRPT2* and LOH in tumors. Parathyroid tumors and matched leukocytes were obtained with informed consent in direct connection to surgery at the Karolinska Hospital. Tumor samples 1–9 and 11–48 were from individuals with a sporadic form of the disease and no personal or family history of MEN1, HPT-JT or other familial forms of 1°HPT. Tumor sample 10 was from a member of kindred-06, who was affected with FIHP linked to 1q⁹. Following the procedure and criteria previously described for tumor cases 1–30 (ref. 11), we confirmed that tumor samples 31–48 collected here were cystic parathyroid adenomas. By histopathological examination of representative sections from the frozen tumors, we confirmed that all samples used contained a sufficient proportion of tumor cells for DNA analyses (that is, >70%).

letter

We screened *HRPT2* for mutations by sequencing the coding region in all 48 tumors (primers and conditions are available on request). We designed the primers to detect mutations in the coding region as well as at the exon-intron junctions. We carried out cycle-sequencing reactions using the BigDye Terminating cycle sequencing kit (Perkin Elmer). Reactions were separated either using an ABI 377 automated sequencer or a 3700 Capillary DNA Analyzer (PE Applied Biosystems).

We genotyped 48 matched blood and tumor DNA samples using seven microsatellite markers located within the critical region encompassing *HRPT2* (Fig. 1). The typed loci included *cen-D1S222-D1S461-D1S542-HRPT2-D1S412-D1S2794-D1S2840-D1S2622-tel*. In addition, we genotyped tumor samples 31–48 for three microsatellites at the *MEN1* locus in 11q13: *cen-(D1S4946/MEN1)-D1S493-D1S4937-tel*. For tumor samples 1–30, LOH analyses of 11q13 have been previously published¹¹. We analyzed the markers using fluorescence detection, and determined the LOH status both visually and by calculating the peak ratios between the constitutional and tumor alleles.

Accession numbers. C1orf28, AF312865; Cdc73p, NP_013522.

Note: Supplementary information is available on the Nature Genetics website.

Acknowledgments

We gratefully acknowledge the selfless participation of the family members in these studies; the hours of clinical time devoted to these studies by M. Leppert, G. Pidworny, O.H. Clark, S. Kytölä, E. Korpi-Hyövähti, C.J. Lips, L.E. Mallette, R. van der Luijt, G.J. Fleuren, L. Barros, V. Leino, M.M. Loureiro, M.C. Pereira, L. Ruas, J. Sampson, M.A. Santos, L.G. Sobrinho, A. Hattersley, R. Paisley, M.H. Wheeler, G. Talpos, I. Sali, D. Finat, M.C. Skarulis and N. Thompson; and the expert technical assistance of K. Dietrich, A. Pole, C. Markey, D. F. Lutz, M.C. Jackson, E. Eddings, G.D. Tran, J. Booth, A.N. Tkachuk and J. Mestre. This work was supported in part by grants from The Swedish Cancer Foundation, the Torsten and Ragnar Söderberg Foundations, the Cornell Foundation and the Gustav V Jubilee Foundation (C.L.), US National Institutes of Health, US National Center for Research Resources Public Health Service Research Grant, the American Cancer Society (M.R.H.), The Dykstra Foundation and the US Public Health Service (C.E.J.), Medical Research Council, U.K. (A.M.K., P.D.L., B.H., A.A.P. and R.V.T.), Rhodes Trust, U.K. (P.D.L.) and Liga Portuguesa Contra o Cancro Instituto Portugues de Oncologia de Francisco Gentil, Portugal (B.M.C.).

Competing interests statement

The authors declare that they have no competing financial interests.

Received 4 September; accepted 24 October 2002.

1. Jackson, C.E. et al. Hereditary hyperparathyroidism and multiple ossifying jaw fibromas: a clinically and genetically distinct syndrome. *Surgery* **108**, 1006–1012; discussion 1012–1013 (1990).

2. Wassif, W.S. et al. Genetic studies of a family with hereditary hyperparathyroidism-jaw tumour syndrome. *Clin. Endocrinol. (Oxf)* **50**, 191–196 (1999).
3. Kennett, S. & Pollick, H. Jaw lesions in familial hyperparathyroidism. *Oral Surg. Oral Med. Oral Pathol.* **31**, 502–510 (1971).
4. Eversole, L.R., Leider, A.S. & Nelson, K. Ossifying fibroma: a clinicopathologic study of sixty-four cases. *Oral Surg. Oral Med. Oral Pathol.* **60**, 505–511 (1985).
5. Szabo, J. et al. Hereditary hyperparathyroidism-jaw tumor syndrome: the endocrine tumor gene *HRPT2* maps to chromosome 1q21-q31. *Am. J. Hum. Genet.* **56**, 944–950 (1995).
6. Teh, B.T. et al. Autosomal dominant primary hyperparathyroidism and jaw tumor syndrome associated with renal hamartomas and cystic kidney disease: linkage to 1q21-q32 and loss of the wild type allele in renal hamartomas. *J. Clin. Endocrinol. Metab.* **81**, 4204–4211 (1996).
7. Haven, C.J. et al. A genotypic and histopathological study of a large Dutch kindred with hyperparathyroidism-jaw tumor syndrome. *J. Clin. Endocrinol. Metab.* **85**, 1449–1454 (2000).
8. Hobbs, M.R., Rosen, I.B. & Jackson, C.E. Revised 14.7-cM locus for the hyperparathyroidism-jaw tumor syndrome gene, *HRPT2*. *Am. J. Hum. Genet.* **70**, 1376–1377 (2002).
9. Teh, B.T. et al. Familial isolated hyperparathyroidism maps to the hyperparathyroidism-jaw tumor locus in 1q21-q32 in a subset of families. *J. Clin. Endocrinol. Metab.* **83**, 2114–2120 (1996).
10. Williamson, C. et al. Mapping the gene causing hereditary primary hyperparathyroidism in a Portuguese kindred to chromosome 1q22-q31. *J. Bone Miner. Res.* **14**, 230–239 (1999).
11. Villablanca, A. et al. Genetic and clinical characterization of sporadic cystic parathyroid tumours. *Clin. Endocrinol. (Oxf)* **56**, 261–269 (2002).
12. Jackson, C.E. & Boonstra, C.E. The relationship of hereditary hyperparathyroidism to endocrine adenomatosis. *Am. J. Med.* **43**, 727–734 (1967).
13. Dinnes, J.S., Greenwood, R.H., Jones, J.H., Walker, D.A. & Williams, E.D. Parathyroid carcinoma in familial hyperparathyroidism. *J. Clin. Pathol.* **30**, 966–975 (1977).
14. Hobbs, M.R. et al. Hyperparathyroidism-jaw tumor syndrome: the *HRPT2* locus is within a 0.7-cM region on chromosome 1q. *Am. J. Hum. Genet.* **64**, 518–525 (1999).
15. Cavaco, B.M. et al. The hyperparathyroidism-jaw tumour syndrome in a Portuguese kindred. *QJM* **94**, 213–222 (2001).
16. Simonds, W.F. et al. Familial isolated hyperparathyroidism: clinical and genetic characteristics of 36 kindreds. *Medicine (Baltimore)* **81**, 1–26 (2002).
17. Sood, R. et al. Cloning and characterization of 13 novel transcripts and the human *RGS8* gene from the 1q25 region encompassing the hereditary prostate cancer (*HPC1*) locus. *Genomics* **73**, 211–222 (2001).
18. Shi, X. et al. Cdc73p and Paf1p are found in a novel RNA polymerase II-containing complex distinct from the Srbp-containing holoenzyme. *Mol. Cell Biol.* **17**, 1160–1169 (1997).
19. Kerkman, K. & Lehman, N. Genome-wide expression analysis of a *Saccharomyces cerevisiae* strain deleted for the Tup1p-interacting protein Cdc73p. *Curr. Genet.* **39**, 284–290 (2001).
20. Pokholok, D.K., Hannett, N.M. & Young, R.A. Exchange of RNA polymerase II initiation and elongation factors during gene expression in vivo. *Mol. Cell* **9**, 799–809 (2002).
21. Thakker, R.V. et al. Association of parathyroid tumors in multiple endocrine neoplasia type 1 with loss of alleles on chromosome 11. *N. Engl. J. Med.* **321**, 1968–1972 (1989).
22. Bystrom, C. et al. Localization of the *MEN1* gene to a small region within chromosome 11q13 by deletion mapping in tumors. *Proc. Natl Acad. Sci. USA* **87**, 1968–1972 (1990).
23. Friedman, E. et al. Allelic loss from chromosome 11 in parathyroid tumors. *Cancer Res.* **52**, 6804–6809 (1992).
24. Marx, S.J. Hyperparathyroid and hypoparathyroid disorders. *N. Engl. J. Med.* **343**, 1863–1875 (2000).
25. Kruglyak, L., Daly, M.J., Reeve-Daly, M.P. & Lander, E.S. Parametric and nonparametric linkage analysis: a unified multipoint approach. *Am. J. Hum. Genet.* **58**, 1347–1363 (1996).



